

Theory of electro-optic modulation via a quantum dot coupled to a nano-resonator

Arka Majumdar*, Nicolas Manquest, Andrei Faraon and Jelena Vučković

*E. L. Ginzton Laboratory, Stanford University,
Stanford, CA, 94305*

[*arkam@stanford.edu](mailto:arkam@stanford.edu)

Abstract: In this paper, we analyze the performance of an electro-optic modulator based on a single quantum dot strongly coupled to a nano-resonator, where electrical control of the quantum dot frequency is achieved via quantum confined Stark effect. Using realistic system parameters, we show that modulation speeds of a few tens of GHz are achievable with this system, while the energy per switching operation can be as small as 0.5 fJ. In addition, we study the non-linear distortion, and the effect of pure quantum dot dephasing on the performance of the modulator.

© 2010 Optical Society of America

OCIS codes: (250.4110) Modulators; (250.3750) Optical logic devices; (250.5590) Quantum-well, -wire and -dot devices; (350.4238) Nanophotonics and photonic crystals.

References and links

1. Q. Xu, S. Manipatruni, B. Schmidt, J. Shakya, and M. Lipson, "12.5 gbit/s carrierinjection-based silicon micro-ring silicon modulators," *Opt. Express* 15, 430–436 (2007).
2. A. Liu, R. Jones, L. Liao, D. Samara-Rubio, D. Rubin, O. Cohen, R. Nicolaescu, and M. Paniccia, "A high-speed silicon optical modulator based on a metal-oxide-semiconductor capacitor," *Nature* 427, 615–618 (2004).
3. Y. Vlasov, W. M. J. Green, , and F. Xia, "High-throughput silicon nanophotonic deflection switch for on-chip optical networks," *Nat. Photonics* 2, 242–246 (2008).
4. J. L. O'Brien, "Optical quantum computing," *Science* 318, 1567–1570 (2007).
5. A. Politi, M. J. Cryan, J. G. Rarity, S. Yu, and J. L. O'Brien, "Silica-on-silicon waveguide quantum circuits," *Science* 320, 646–649 (2008).
6. D. Englund, A. Faraon, B. Zhang, Y. Yamamoto, and J. Vuckovic, "Generation and transfer of single photons on a photonic crystal chip," *Opt. Express* 15, 5550–5558 (2007).
7. A. Faraon, I. Fushman, D. Englund, N. Stoltz, P. Petroff, and J. Vuckovic, "Dipole induced transparency in waveguide coupled photonic crystal cavities," *Opt. Express* 16, 12154–12162 (2008).
8. D. M. Szymanski, B. D. Jones, M. S. Skolnick, A. M. Fox, D. O'Brien, T. F. Krauss, and J. S. Roberts, "Ultrafast all-optical switching in algaas photonic crystal waveguide interferometers," *Appl. Phys. Lett.* 95(14), 141108–141110 (2009).
9. C. Husko, A. D. Rossi, S. Combrie, Q. V. Tran, F. Raineri, and C. W. Wong, "Ultrafast all-optical modulation in GaAs photonic crystal cavities," *Appl. Phys. Lett.* 94(2), 021111 (2009).
10. N. Hitoshi, Y. Sugimoto, K. Kanamoto, N. Ikeda, Y. Tanaka, Y. Nakamura, S. Ohkouchi, Y. Watanabe, K. Inoue, H. Ishikawa, and K. Asakawa, "Ultra-fast photonic crystal/quantum dot alloptical switch for future photonic networks," *Opt. Express* 12, 6606–6614 (2004).
11. A. Faraon, A. Majumdar, H. Kim, P. Petroff, and J. Vuckovic, "Fast electrical control of a quantum dot strongly coupled to a nano-resonator," *Phys. Rev. Lett.* 104, 047402 (2010).
12. D. Englund, A. Faraon, A. Majumdar, N. Stoltz, P. Petroff, and J. Vuckovic, "An optical modulator based on a single strongly coupled quantum dot - cavity system in a p-i-n junction," *Opt. Express* 17, 18651–18658 (2009).
13. D. A. B. Miller, "Device requirements for optical interconnects to silicon chips," *Proc. IEEE* 97, 1166–1185 (2009).

14. D. Englund, A. Faraon, I. Fushman, N. Stoltz, P. Petroff, and J. Vuckovic, "Controlling cavity reflectivity with a single quantum dot," *Nature* 450, 857-861 (2007).
15. C. W. Gardiner and P. Zoller, *Quantum Noise*. (Springer-Verlag, 2005).
16. E. Waks and J. Vuckovic, "Dipole induced transparency in drop filter cavity-waveguide systems," *Phys. Rev. Lett.* 96, 153601 (2006).
17. I. Fushman, D. Englund, A. Faraon, N. Stoltz, P. Petroff, and J. Vuckovic, "Controlled phase shifts with a single quantum dot," *Science* 320, 769-772 (2008).
18. J. Liu, M. Beals, A. Pomerene, S. Bernardis, R. Sun, J. Cheng, L. C. Kimerling, and J. Michel, "Waveguide-integrated, ultralow-energy gesi electro-absorption modulators," *Nat. Photonics* 2, 433-437 (2008).
19. Q. Xu, D. Fattal, and R. G. Beausoleil, "Silicon microring resonators with 1.5-um radius," *Opt. Express* 16, 4309-4315 (2008).

1. Introduction

During the past decade there has been an extensive effort towards building solid state optical devices with micron-scale footprint. The main drive behind this research is the development of optical networks for chip to chip interconnects [1-3] and optical quantum information processing [4-7]. In these networks, modulators play an essential role in sending and routing information. Most of the micron-scale modulators fabricated so far are based on either classical effects or collective quantum effects [8-10]. However, a few papers recently published [11, 12] show that a single quantum emitter can be deterministically used to control the transmission of a beam of light.

The reduction in operating power is one of the most important reasons for miniaturizing optical components down to scales where the active component is represented by a single quantum emitter. Currently, one of the main bottlenecks in developing high speed electronic devices is the large loss in the metal interconnect at high frequency [13]. The development of light switches operating at levels of just a few quanta of energy may be a solution. At the same time, these devices represent a new tool in the rapidly developing toolbox of quantum technologies.

Our recent demonstration of electro-optic switching at the quantum limit is based on a single InAs quantum dot (QD) embedded in a GaAs photonic crystal resonator. The system operates in the strong coupling regime of cavity quantum electrodynamics (CQED) [14]. The control of the quantum dot is achieved by changing the quantum dot frequency via the quantum confined Stark effect [11]. In this paper we theoretically analyze the performance of this type of electro-optic modulator. We study its maximum achievable modulation speed, linearity, step response and power requirement. Lastly, we investigate how pure QD dephasing affects the modulator performance.

2. Modulation method and analysis

The Master equation describing the dynamics of a coherently driven single QD (lowering operator $\sigma = |g\rangle\langle e|$; where $|g\rangle$ and $|e\rangle$ are the ground and the excited states of the QD) coupled to a single cavity mode (with annihilation operator a) is given by ($\hbar = 1$) [15]

$$\frac{d\rho}{dt} = -i[H, \rho] + \kappa\mathcal{L}[a] + \gamma\mathcal{L}[\sigma] + \frac{\gamma_d}{2}(\sigma_z\rho\sigma_z - \rho) \quad (1)$$

where ρ is the density matrix of the coupled cavity/QD system; 2γ and 2κ are the QD spontaneous emission rate and the cavity population decay rate respectively; γ_d is the pure dephasing rate of the QD; $\sigma_z = [\sigma^\dagger, \sigma]$. $\mathcal{L}[D]$ is the Lindblad operator corresponding to a collapse operator D . This is used to model the incoherent decays and is given by:

$$\mathcal{L}[D] = 2D\rho D^\dagger - D^\dagger D\rho - \rho D^\dagger D \quad (2)$$

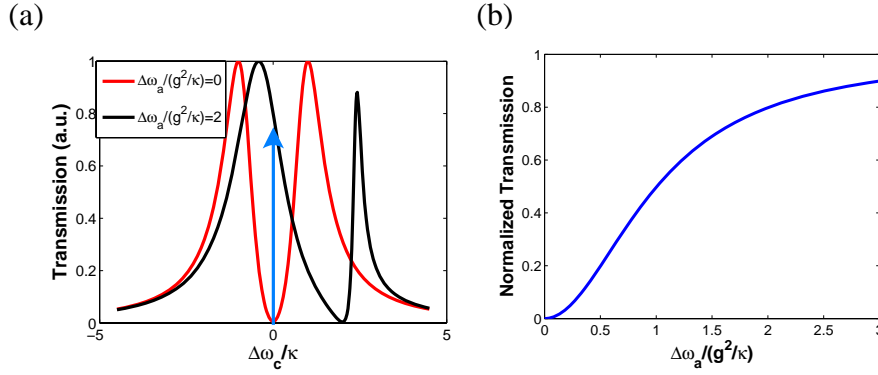


Fig. 1. (a) Transmission spectra of coupled cavity-QD system for two different detunings. The blue arrow shows the wavelength of the laser whose transmission is being modified. (b) Normalized steady state transmission with different QD detunings. The laser is resonant with the cavity. We used the following parameters: $g/2\pi = \kappa/2\pi = 20$ GHz; $\gamma = \kappa/80$; the pure dephasing rate is assumed to be zero for this analysis ($\gamma_d/2\pi = 0$).

H is the Hamiltonian of the system without considering the losses and is given by (in rotating wave approximation, where the frame is rotating with the driving laser frequency)

$$H = \Delta\omega_c a^\dagger a + \Delta\omega_a \sigma^\dagger \sigma + ig(a^\dagger \sigma - a \sigma^\dagger) + \Omega(a + a^\dagger) \quad (3)$$

where $\Delta\omega_c = \omega_c - \omega_l$ and $\Delta\omega_a = \omega_a - \omega_l$ are respectively the cavity and dot detuning from the driving laser; ω_c , ω_a and ω_l are the cavity resonance, the QD resonance and the driving laser frequency respectively; Ω is the Rabi frequency of the driving laser and is given by $\vec{\mu} \cdot \vec{E}$, where $\vec{\mu}$ is the dipole moment of the transition driven by the laser and \vec{E} is the electric field of the laser inside the cavity at the position of the QD; and g is the interaction strength of the QD with the cavity.

Using the identity $\langle \dot{\hat{O}} \rangle = Tr(\hat{O}\dot{\rho})$ for an operator \hat{O} and a density matrix ρ in Eq. (1), we find the following Maxwell-Bloch equations (MBEs) for the coupled cavity/QD system (assuming the laser is resonant with the cavity frequency, i.e., $\Delta\omega_c = 0$):

$$\frac{d\langle X \rangle}{dt} = A\langle X \rangle + i\Omega B \quad (4)$$

$$\frac{d\langle Y \rangle}{dt} = C\langle Y \rangle + i\Omega D\langle X \rangle \quad (5)$$

where

$$X = [a \quad \sigma \quad a^\dagger \quad \sigma^\dagger]^T \quad (6)$$

$$Y = [a^\dagger a \quad \sigma^\dagger \sigma \quad a^\dagger \sigma \quad a \sigma^\dagger]^T \quad (7)$$

$$A = \begin{bmatrix} -\kappa & g & 0 & 0 \\ -g & \Gamma & 0 & 0 \\ 0 & 0 & -\kappa & g \\ 0 & 0 & -g & \Gamma^* \end{bmatrix} \quad (8)$$

$$B = [-1 \quad 0 \quad 1 \quad 0]^T \quad (9)$$

$$C = \begin{bmatrix} -2\kappa & 0 & g & g \\ 0 & -2\gamma & -g & -g \\ -g & g & \Gamma - \kappa & 0 \\ -g & g & 0 & \Gamma^* - \kappa \end{bmatrix} \quad (10)$$

$$D = \begin{bmatrix} 1 & 0 & -1 & 0 \\ 0 & 0 & 0 & 0 \\ 0 & 1 & 0 & 0 \\ 0 & 0 & 0 & -1 \end{bmatrix} \quad (11)$$

where $\Gamma = -(\gamma + \gamma_d + i\Delta\omega_a)$. In deriving the MBEs, we assume that under low excitation, the system stays mostly in the lowest manifolds (single quantum of energy) and hence $\langle a\sigma_z \rangle \approx -\langle a \rangle$ and $\langle a^\dagger a\sigma_z \rangle \approx -\langle a^\dagger a \rangle$ [16].

When operating as a modulator, the cavity/QD system modulates the transmission of the laser driving the cavity (laser amplitude E and frequency ω_l). The system is modulated using an electrical signal which changes the QD resonance frequency via quantum confined Stark effect (QCSE). In our analysis, we assume that the optical signal is always resonant with the bare cavity ($\omega_l = \omega_c$) and only the QD resonance frequency changes. We note that applying electric field across the QD reduces the overlap between the electron and the hole wavefunctions and thus reduces the dipole moment of the QD and the coherent coupling strength g . However the reduction in g is due to the change in the spatial overlap of the eigen-states of the perturbed Hamiltonian (the Hamiltonian describing the confining potential of the QD), while the change in the QD resonance frequency is due to the modification of eigenvalues of the perturbed Hamiltonian. The perturbation in eigen-states due to QCSE is a higher order effect than the change in eigenvalues. Hence the reduction in g is much less prominent than the change in the QD resonance frequency and we preserve strong coupling even with the applied electric field [11]. However, there is a finite probability for the electron or the hole to tunnel out of the QD, when a large electric field E_{tun} is applied. For successful operation of the electro-optic modulator, the applied electric field must be smaller than E_{tun} and in this paper, we assume that this condition is satisfied.

The system operates in strong coupling regime when $g \gg \kappa, \gamma$. In this regime, when the quantum dot and the cavity are resonant, the optical system has a split resonance (in contrast to a single Lorentzian), as shown in Fig. 1(a). The detuning of the quantum dot due to the application of an electric field causes dramatic changes in the transmission spectrum of the optical system. This directly affects the transmitted intensity of a laser tuned at the bare cavity resonance [shown by an arrow in Fig. 1(a)]. Figure 1(b) shows the steady-state transmission (normalized by the transmission through an empty cavity) for different values of QD-cavity detuning. This has been derived by solving the MBEs [Eqs. (4), (5)] at steady-state (in absence of pure dephasing, i.e., $\gamma_d/2\pi = 0$), which gives that the ratio of the maximum to the minimum transmission through the cavity is $(1 + g^2/\kappa\gamma)^2$.

The performance of the modulator is analyzed by numerically solving the MBEs, and thus deriving the time evolution of the system. An alternative method involves numerically solving the exact Master equation [Eq. (1)]. Both methods give us exactly the same solutions and we report only the result obtained from the MBEs, as this method is much faster and computationally less demanding. To relate our theory to current state of the art technology where values of $\kappa/2\pi = g/2\pi \approx 20$ GHz ($\kappa/2\pi = 20$ GHz corresponds to a cavity quality factor of ~ 8000) can be easily achieved [14], we mainly analyze the system performance for both $\kappa/2\pi$ and $g/2\pi$ ranging between 10 to 40 GHz.

3. Frequency response

The foremost criterion of a good electro-optic modulator is its speed of operation. In this electro-optic modulator, the modulation speed is determined by two different time scales. One time scale depends on how fast the QD can be modulated by applying an electric field. This depends on the drift velocity of electrons and holes in the semiconductor, and the electrical capacitance of the modulator. As the active area of the modulator is very small (dimensions of

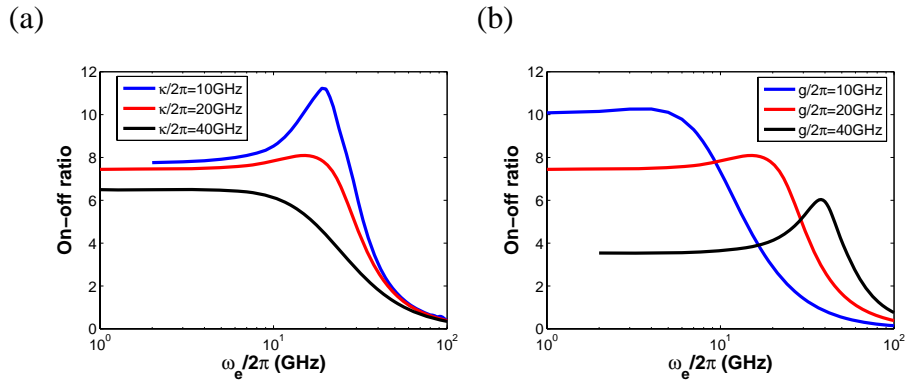


Fig. 2. The frequency response of the switch for different (a) κ . ($g/2\pi$) is kept constant at 20 GHz and (b) g . ($\kappa/2\pi$) is kept constant at 20 GHz. For both simulations $\Omega = 1$ GHz; $\Delta\omega_0/2\pi = 10$ GHz; $\gamma_d/2\pi = \gamma/2\pi = 0.1$ GHz.

a QD $\sim 10 \times 10nm^2$), this time scale is extremely short and thus does not limit the modulator speed. The other time scale is due to the optical bandwidth of the system, i.e., the finite bandwidths of the cavity spectrum and the dip induced by the strong coupling of the dipole to the cavity. The cavity has a finite bandwidth, which limits how fast the modulator can operate. This optical bandwidth limits the speed of operation of the electro-optical modulator described here. To estimate the bandwidth of modulation, one can consider the cavity transmission spectrum [as shown by the red line in Fig. 1(a)] as the filter response of the modulator; for successful operation, the pulse bandwidth should not exceed the splitting obtained due to the strong coupling. Following this argument, the bandwidth of the pulse that can be modulated via this electro-optic modulator is approximately g^2/κ .

However, to obtain the modulation speed more rigorously, we apply a sinusoidal change in the QD resonance frequency: $\Delta\omega_a(t) = \frac{1}{2}\Delta\omega_0(1 - \cos(\omega_e t))$; where $\Delta\omega_0$ is the maximum detuning of the QD resonance (this is proportional to the amplitude of the electrical signal applied to tune the QD) and ω_e is the frequency of the modulating electrical signal and hence also the frequency of the change in the QD resonance. The system performance is determined by analyzing the change in the cavity output (i.e. $\kappa\langle a(t)^\dagger a(t) \rangle$) as a function of ω_e . The on/off ratio is defined as the ratio of the maximum to minimum cavity output during sinusoidal driving. The Rabi frequency Ω of the driving laser is chosen such that the QD is not saturated. The effect of free carriers generation in semiconductor surrounding the QD by two photon absorption of the driving laser is not included in our analysis as at low Ω (that is, at low intensity of the driving laser) this effect is very small. The pure dephasing rate $\gamma_d/2\pi$ of the QD is assumed to be 0.1 GHz.

Figure 2 shows the on-off ratio of the output signal as a function of frequency of modulating signal for different κ and g . We observe that the modulator behaves like a second order low pass filter with a roll-off of -20 dB/decade. Figure 3 shows the cut-off frequency and the on-off ratio at low frequency as a function of different g and κ . The cut-off frequency of the filter increases with the coupling strength g . Similarly, reduction in κ increases the cut-off frequency. However when $\kappa < g$, the change in cut-off frequency is not significant and g plays the dominant role. At the same time, the on-off ratio decreases with g , which occurs because we kept the maximum detuning $\Delta\omega_0/2\pi$ fixed at 5 GHz. By increasing $\Delta\omega_0/2\pi$ the on-off ratio can be increased for higher values of g .

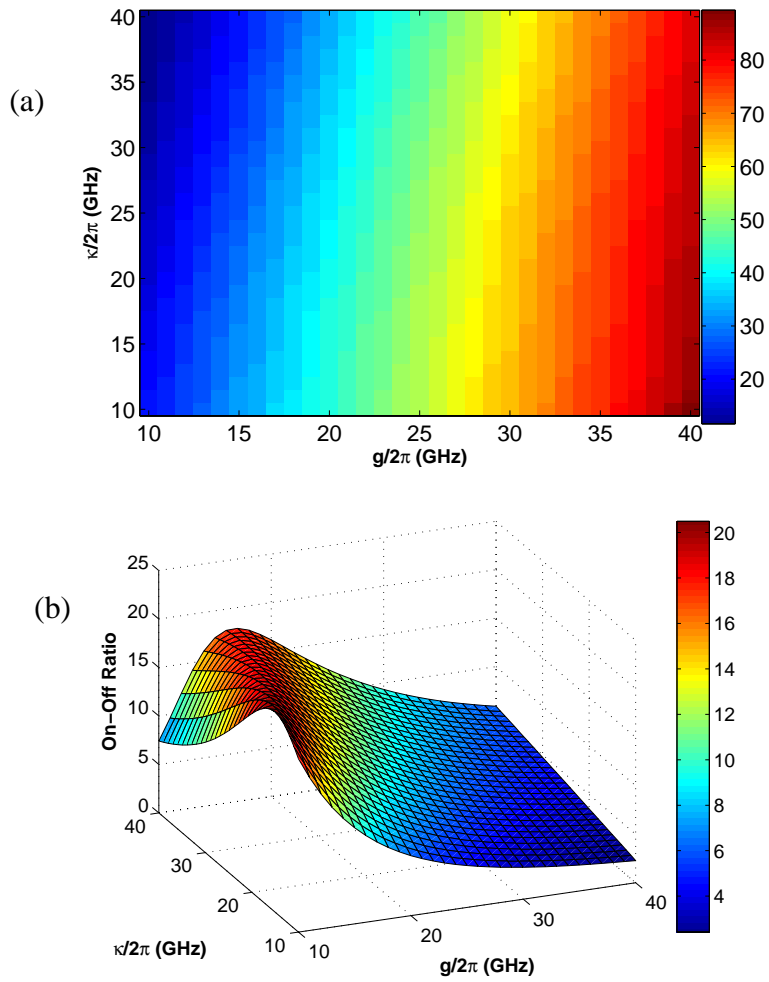


Fig. 3. (a) Cut-off frequency of the modulator as a function of g and κ . In the color scheme, the maximum cutoff frequency of ~ 90 GHz is red and the minimum cut-off frequency of ~ 10 GHz is blue; (b) On-off ratio of the modulator at a modulating frequency of $\omega_e/2\pi = 5$ GHz as a function of g and κ . For both plots $\Delta\omega_0/2\pi = 5$ GHz; $\gamma_d/2\pi = 0.1$ GHz; $\Omega = 1$ GHz.

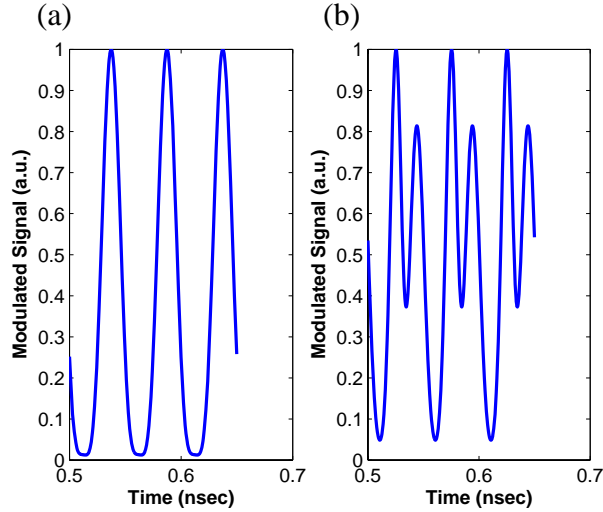


Fig. 4. Normalized output signal for two different maximal QD detunings $\Delta\omega_0$. (a) $\Delta\omega_0/2\pi = 2$ GHz. (b) $\Delta\omega_0/2\pi = 40$ GHz. For both simulations the frequency of the electrical signal is $\omega_e/2\pi = 20$ GHz, $\kappa/2\pi = g/2\pi = 20$ GHz and $\Omega = 1$ GHz.

4. Nonlinear distortion of signal

Another important property of good modulators is that the modulated optical output should closely resemble the shape of the modulating electrical signal. If the modulator does not operate in the linear regime, the output signal contains spurious higher harmonics. Figure 4 shows the optical output signal for two different values of maximal QD detuning $\Delta\omega_0$. For small values of the electrical input (i.e., for small $\Delta\omega_0$), the output follows exactly the variation of the QD resonance frequency, as shown in Fig. 4(a). However, distortions appear for higher amplitudes of $\Delta\omega_0$ [Fig. 4(b)]. Here we observe ripples at a frequency different from the modulating frequency ω_e . These ripples do not arise only because of the finite bandwidth of the system, but are also due to the nonlinearity of the system with respect to $\Delta\omega_0$. More detailed analysis of these ripples are described below, when we analyze the step response of the modulator. The value of $\Delta\omega_0$ also affects the visibility of the modulated signal. The on-off ratio (i.e., the desired output) is proportional to the first harmonic of the modulated output signal. Figure 5 shows the ratio of second and third harmonics to the first harmonic of the output signal as a function of $\Delta\omega_0$. As expected, the higher order harmonics increase with increase in QD detuning $\Delta\omega_0$.

We note that by employing a differential detection method, one can get rid of the even order harmonics. For differential detection, one uses two electro-optic modulators, but the electrical signals applied to the modulators are out of phase. Let us assume the desired signal, when the modulator is in linear regime, is $x(t) = A\sin(\omega t)$. Due to nonlinearity the distorted signal is $x_d(t) = A_1\sin(\omega t) + A_2\sin^2(\omega t) + A_3\sin^3(\omega t) + \dots$, where A_1, A_2, A_3 are the amplitudes of different harmonics. In differential detection, we apply two out of phase signals and then subtract the modulated optical signals to remove the even order harmonics, which are unaffected by the phase change. Hence the performance of the modulator is primarily determined by the third order harmonics.

5. Step response

The step response gives information about both the bandwidth of the system and the nonlinear distortion. To analytically calculate the step response we consider two situations: (1) when the

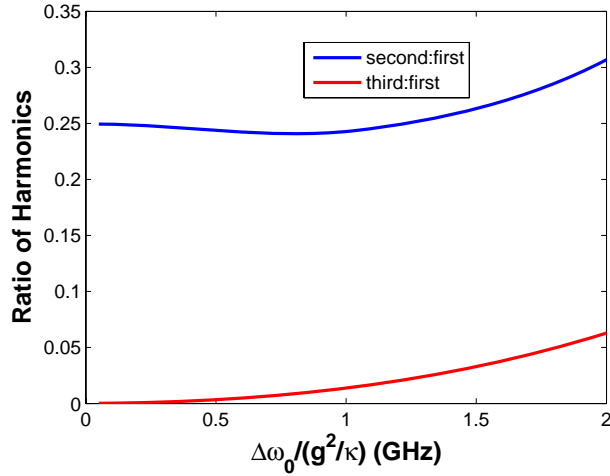


Fig. 5. Ratio of the second and third harmonic to the first harmonic of the modulated signal, as a function of the maximum frequency shift of the QD, scaled by a factor of g^2/κ . The first harmonic is proportional to the actual signal. For the simulation we assumed that the modulation is working in the passband ($\omega_e/2\pi = 20$ GHz); $\kappa/2\pi = g/2\pi = 20$ GHz and the dephasing rate $\gamma_d/2\pi = 0$.

electrical signal goes from on to off (that is the QD detuning goes from $\Delta\omega_0 \rightarrow 0$); and (2) when the electrical signal goes from off to on (that is the QD detuning goes from $0 \rightarrow \Delta\omega_0$). For low excitation and small dephasing rate, the average value of cavity output $\kappa|\langle a(t)^\dagger a(t) \rangle|$ is approximately given by $\kappa|\langle a(t) \rangle|^2$, where $\langle a(t) \rangle$ is

$$\langle a(t) \rangle_{\Delta\omega_0 \rightarrow 0} = r(0)e^{-\alpha(0)t} \cos(\beta(0)t + \phi(0)) + SS(0) \quad (12)$$

and

$$\langle a(t) \rangle_{0 \rightarrow \Delta\omega_0} = r(\Delta\omega_0)e^{-\alpha(\Delta\omega_0)t} \cos(\beta(\Delta\omega_0)t + \phi(\Delta\omega_0)) + SS(\Delta\omega_0) \quad (13)$$

where the switching happens at $t = 0$ and

$$\begin{aligned} \alpha(\omega) &= \frac{\kappa + \gamma + i\omega}{2} \\ \beta(\omega) &= \frac{\sqrt{4g^2 - (\kappa - \gamma - i\omega)^2}}{2} \\ SS(\omega) &= \frac{i\Omega(\gamma + i\omega)}{g^2 + \kappa(\gamma + i\omega)} \\ \phi(\omega) &= \tan^{-1} \left(\frac{\alpha(\omega)}{\beta(\omega)} \right) \\ r(0) &= \frac{SS(\Delta\omega_0) - SS(0)}{\cos(\phi(0))} \\ r(\Delta\omega_0) &= \frac{SS(0) - SS(\Delta\omega_0)}{\cos(\phi(\Delta\omega_0))} \end{aligned}$$

Figure 6 shows the step response of the modulator. The numerical simulation of MBEs and the analytical expression for the step response show excellent agreement. We see the oscillations

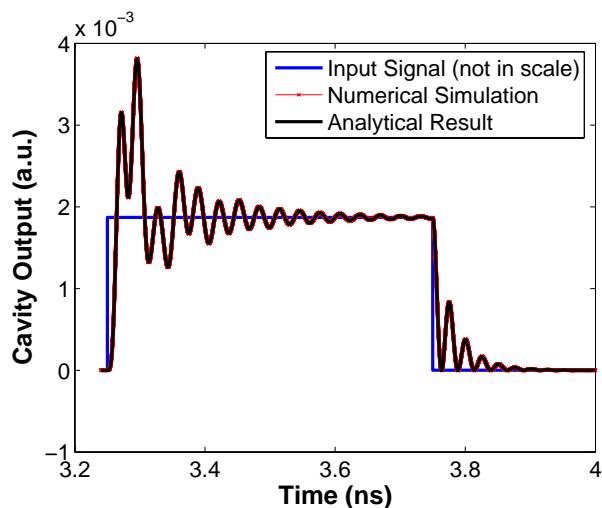


Fig. 6. Step response of the single QD electro-optic modulator. The parameters used for the simulation are: $\kappa/2\pi = 5$ GHz; $g/2\pi = 20$ GHz; $\Delta\omega_0/2\pi = 20$ GHz; $\Omega = 1$ GHz.

in step response because the system needs finite time to relax. Due to non-linearity of the system, this relaxation time depends on $\Delta\omega_0$. Hence in Fig. 4 we observe ripples only for high values of $\Delta\omega_0$.

Following previous analysis, we observe that with high amplitude of electrical signal ($\Delta\omega_0$), the on-off ratio of the modulator increases, but the modulated signal becomes distorted. In fact, when QD-cavity coupling g is large, one needs high $\Delta\omega_0$ to achieve good on-off ratio (Fig. 3). However, it should be noted that in a system with high g , the amplitude of electrical signal causing distortion is also high. Figure 7 shows the ratio between the third and first harmonic of the modulated signal for different g and $\Delta\omega_0$. We observe that for same amplitude of electrical signal (i.e., $\Delta\omega_0$), the distortion is larger for a system with smaller g .

6. Switching power

For most of the modern optoelectronic devices, the energy required per switching operation is one of the most important figures of merit [13]. For the type of devices presented in this paper, the fundamental limit for the control energy per switching operation is given by the energy density of the electric field required to detune the QD inside the active volume. To estimate the control energy we use the experimental parameters as presented in [11]. When the electrode is placed laterally at a distance of $1\mu\text{m}$, the active region of the cavity/QD system has a volume of $V \sim 1\mu\text{m} \times 1\mu\text{m} \times 200\text{nm}$. Since the electric field to tune the quantum dot is on the order of $F \sim 5 \times 10^4$ V/cm, the energy per switching operation is on the order of $E = \epsilon_0 \epsilon_r F^2 V / 2 \sim 0.5$ fJ ($\epsilon_r \sim 13$). This translates into an operating power of $\sim 5\mu\text{W}$ at 10 GHz. The same order of magnitude estimation is obtained by modeling the device as a parallel plate capacitor with width $w \sim 1\mu\text{m}$, thickness $t \sim 200\text{nm}$ and spacing $L \sim 1\mu\text{m}$ and taking into account fringing effects. Since the energy consumption has a quadratic dependence on the applied voltage, the operating power can be lowered significantly by bringing the electrode closer to the quantum dot. In case the active volume could be reduced to the size of the quantum dot itself ($\sim 25 \times 25 \times 25 \text{ nm}^3$), the switching energy can be lowered below 0.1 aJ. These energy scales are of the same order of magnitude as all other optical switching devices operating at single photon level [14, 17], and are orders of magnitude lower than the current state of the art electro-optic modulators [18, 19].

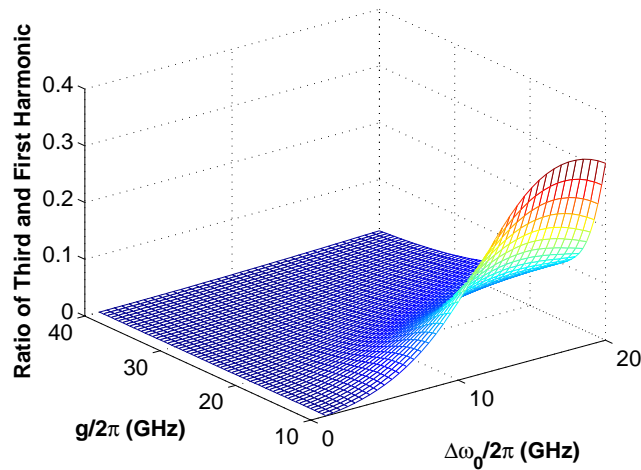


Fig. 7. Ratio between the third and first harmonic of the modulated signal for different QD-cavity coupling g and maximum QD detuning $\Delta\omega_0$. The cavity decay rate $\kappa/2\pi = 20$ GHz and the modulation frequency $\omega_e/2\pi = 5$ GHz.

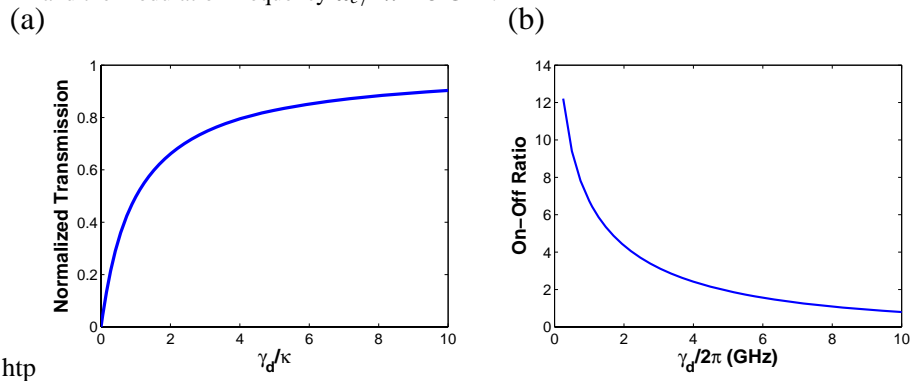


Fig. 8. (a) Normalized steady state transmission of the laser resonant with the dot (i.e., $\Delta\omega_a = 0$) with pure dephasing rate $\gamma_d/2\pi$. Parameters used are: $g/2\pi = \kappa/2\pi = 20$ GHz; $\gamma = \kappa/80$; (b) On-off ratio of the modulated signal as a function of the dephasing rate, for $\kappa/2\pi = g/2\pi = 20$ GHz. The modulation frequency $\omega_e/2\pi = 5$ GHz and the amplitude of the change in resonance frequency $\Delta\omega_0/2\pi = 10$ GHz.

However, this electro-optic modulator cannot be used to modulate high power optical signal, as high optical power will saturate the QD.

7. Effect of dephasing of QD

One of the major problems in CQED with a QD is the dephasing of the QD, caused by interaction of the QD with nearby nuclei and phonons. The dip in transmission through the cavity in presence of a coupled QD is caused by the destructive interference of the incoming light and the light absorbed and re-radiated by the QD [16]. Due to the dephasing of the QD, the light scattered from the QD is not exactly out-of-phase with the incoming light. This affects the destructive interference thus causing the cavity to be not fully reflective. Figure 8(a) shows the steady state transmission through a coupled cavity/QD system (normalized by the transmission

through an empty cavity) of a laser resonant with the cavity and the QD, as a function of QD dephasing rate. Hence, the performance of the modulator also suffers because of dephasing. Figure 8(b) shows the on-off ratio as a function of the dephasing rate $\gamma_d/2\pi$ of the QD. As expected the on-off ratio falls off with increased dephasing rate.

8. Conclusion

We have performed the detailed analysis of the performance of an electro-optic modulator where the modulation is provided by a single QD strongly coupled to a cavity. We have shown that a modulation speed of 40 GHz can be achieved for realistic system parameters ($\kappa/2\pi = g/2\pi = 20$ GHz) with a control energy of the order of 0.5 fJ. This type of fast and low control energy modulator may constitute an essential building block of future nano-photonic networks.

Acknowledgement

The authors gratefully acknowledge financial support provided by the National Science Foundation, Army Research Office and Office of Naval Research. A.M. was supported by the Stanford Graduate Fellowship (Texas Instruments fellowship).